applied sciences

MDPI

Article

Effects of Ca^{2+} Ions on the Localized Corrosion of Carbon Steel Influence of the Associated Anion

Verónica Viviana Acosta [1,2] and Gustavo Luis Bianchi [2,3,*]

[1] Department of Chemical Engineering, Faculty of Engineering, National University of Patagonia San Juan Bosco, Comodoro Rivadavia U9000, Argentina; acosta_veronica@unpata.edu.ar
[2] National Scientific and Technical Research Council (CONICET), Buenos Aires 1430, Argentina
[3] Energy and Environmental Innovation Group, Malvinas Institute, Faculty of Engineering, National University of La Plata, Diagonal 80 No. 372, La Plata 1900, Argentina
* Correspondence: gustavo.bianchi@ing.unlp.edu.ar

Abstract: The corrosion rate of carbon steel under the attack of electrolytic mediums saturated by CO_2 at a working temperature of 65 °C under dynamic conditions is studied in this paper. The effect of Ca^{2+} ions on corrosion rates and their dependency on the associated anion (Cl^- or CO_3^{2-}) with respect to the Ca^{2+} cation and Na^+ are also assessed. A potentiostat/galvanostat associated with a rotor stator in an AISI 1040 steel-ring configuration, rotating at 600 rpm, was used. A linear polarization-resistance technique was applied to calculate the corrosion rate. It is found that the corrosion rate depends not only on the presence of Ca^{2+}, but also on the salt anion added to the electrolytic medium. There was a strong inhibitory effect of the corrosion in the presence of Ca^{2+} in chloride-free mediums because of an ankerite deposition with a lower solubility compared to siderite. Moreover, it was observed that, even if the corrosion rate increased together with the Cl^- concentration, its value depended on the cation introducing the anion. It was higher when Cl^- was associated with Na^+ compared to when it was associated with Ca^{2+}. We found the following decreasing order in the carbon steel corrosion rate: 2% NaCl + 1380 ppm $CaCl_2$ > 2% NaCl > 2% NaCl + 1360 ppm Na_2CO_3 > 2% NaCl + 1.25 g/L $CaCO_3$ > 1450 ppm of NaCl > 1380 ppm $CaCl_2$ > 1360 ppm Na_2CO_3 > 500 ppm $CaCl_2$ > 424 ppm Na_2CO_3 >> 1.250 g/L $CaCO_3$.

Keywords: CO_2 corrosion; steel corrosion; corrosion scale; complex carbonate; Ca^{2+} ions

Citation: Acosta, V.V.; Bianchi, G.L. Effects of Ca^{2+} Ions on the Localized Corrosion of Carbon Steel Influence of the Associated Anion. *Appl. Sci.* **2023**, *13*, 11056. https://doi.org/10.3390/app131911056

Academic Editor: Yeoheung Yun

Received: 3 August 2023
Revised: 14 September 2023
Accepted: 23 September 2023
Published: 8 October 2023

1. Introduction

Carbon steel is one of the most used materials for pipelines in the petrol industry. Corrosion attacks may be uniform or localized, influenced by the aggressive medium in its chemical composition, as well as by the flow conditions and other operating variables. Formation water has a high concentration of both Na^+ and Cl^- ions. It also has Ca^{2+} and Mg^{2+}, among others, which are precursors in precipitate formation and may influence the morphology of corrosion attacks. Moreover, the presence of CO_2 has caused serious problems for this industry, and corrosion under such conditions occurs in oxygen-free environments [1].

$FeCO_3$, (Fe,Ca)CO_3, and $\alpha, \gamma \bullet Fe_2O_3 \bullet H_2O$ [2] are the corrosion products that appear the most frequently in water–oil, water–gas and/or water–oil–gas applications containing CO_2. Generally, these compounds are often considered to provide protection against corrosion [3,4]. These compounds are formed by releasing Fe^{2+} ions during the electrochemical corrosion process and they precipitate when the $[Fe^{2+}] \times [CO_3^{2-}]$ concentration product locally exceeds the solubility limits (Kps) of $FeCO_3$. Calcium, as an element that is widely distributed in the oil industry, may be found as $CaCl_2$ and/or $CaCO_3$ and it favors $CaCO_3$ precipitation in brine formation. Both ferrous carbonate and calcium carbonate precipitations significantly depend on their local saturation degrees in the solution.

Numerous studies have alluded to the effects of $FeCO_3$ in relation to the corrosion rate suppression of carbon steel in CO_2-containing environments [5]. Although few studies assess the effect of Ca^{2+} anions on sweet corrosion [6], many works on Ca^{2+}-rich solutions do not explicitly state the salt added to the simulated medium. Mansoori et al. [6] reviewed the works related to this topic, referring to Ca^{2+} or Mg^{2+} concentrations but with no record of the anion used by the researchers.

Jiang et al. [7] assessed the effect of calcium ions on the pitting corrosion of N80 steel. They worked with 3% NaCl, 4.5% NaCl, and 3.5% NaCl + 1.5% $CaCl_2$ solutions saturated by CO_2 at 57 °C in stagnant and dynamic conditions. They pointed out that the initiation period of pitting corrosion was indicated by an abrupt decrease in the magnitude of the impedance, which was observed at 70 h of immersion in 3% NaCl, at 49 h in 3.5% NaCl + 1.5% $CaCl_2$, and at 23 h in 4.5% NaCl. They concluded that in stagnant conditions without Ca^{2+}, the corrosion rate increased together with the increase in chlorides. However, for solutions with the same Cl^- concentration, the corrosion rate decreased due to the addition of Ca^{2+}. They pointed out that the initiation period of pitting corrosion decreased as the Cl^- concentration increased; however, at the same concentration of this ion, Ca^{2+} prolonged the initiation period [7].

Ding et al. [8] studied the effect of Ca^{2+}, by adding it to the solution as $CaCl_2$, on the CO_2 corrosion of API 5L-X65 steel. They simulated a formation water to which they added 64, 128, 256, and 512 mg/L of Ca^{2+} under stagnant conditions at a 1 MPa partial pressure of CO_2 at 75 °C. They concluded that the corrosion rate increased as the Ca^{2+} ions' concentration increased.

Tavares et al. [9] studied the effects of Ca^{2+} ions on the CO_2 corrosion of API 5L-Gr B steel under stagnant conditions at 80 °C. They obtained measurements using two mediums saturated by NaCl and CO_2 (15 MPa), differentiated by the presence or absence of $CaCO_3$ (0.5 mol/kg), attacking the graduated cylinders for 72, 336, and 672 h. They concluded that the uniform attack was predominant for both solutions, with a preferential dissolution of ferrite. They also reported that the corrosion rate by weight loss decreased over time and it was always lower for the $CaCO_3$ solution. Based on the electrochemical measurements, they concluded that, even though they observed "a lower corrosion potential and a higher polarization resistance" when the medium contained $CaCO_3$, there was a period of depassivation, followed by pit formation after 500 mV (vs. SCE). They pointed out that this occurred because the mixed carbonate was more porous and, thus, more susceptible to Cl^- ion permeability, in comparison to $FeCO_3$ [9].

Esmaeely et al. [10] studied the effect of Ca^{2+} on CO_2 corrosion in a glass cell in stagnant conditions at 0.05 MPa CO_2, 80 °C with 1% *w*/*w* NaCl with different concentrations of Ca^{2+} (between 0 and 10,000 ppm) and an initial concentration of Fe^{2+} of 10 ppm, for a 7-day period. They reported that the corrosion rate decreased over time when the Ca^{2+} concentration varied between 0 and 100 ppm. Based on this, they pointed out that the formation of a protective $FeCO_3$ layer occurred with no significant interference by Ca^{2+}. However, for higher Ca^{2+} concentrations (between 1000 and 10,000 ppm), the corrosion rate was higher.

In a subsequent study, Esmaeely et al. [11] studied the effects of Ca^{2+} ions on the formation and protectiveness of the $FeCO_3$ layer in aqueous solutions for the CO_2 corrosion of G10180 steel. They reported a localized corrosion in the presence of high concentrations, and that Ca^{2+} was responsible for the initiation of localized attacks, rather than Cl^-, since they did not observe any indications of pitting for the Ca^{2+} solution. Moreover, they observed that at 10,000 ppm Ca^{2+} and 600 rpm, there were no indications of pitting.

Mansoori et al. [6] pointed out that, in 1984, Eriksrud and Sontvedt [12] conducted one of the first studies to assess the effects of Ca^{2+} and Mg^{2+}, along with other ions, on the CO_2 corrosion of API 5L X52 steel. They conducted potentiodynamic sweeps for three different Ca^{2+} concentrations, 0, 400, and 1200 ppm, at 20 °C, 1 bar partial pressure of CO_2, over a pH range of 5.80–7.39 for two days. They reached the conclusion that the formation of $FeCO_3$ protective layers enriched with Ca^{2+} led to a drop in the corrosion rate of mild steel.

In the review by Mansoori et al. [6], they mentioned the work of Zhao et al. [13]. They stated that the corrosion rate decreased in the "short term" in the presence of Ca^{2+} and $Mg^{2+;}$ however, there was no special difference for the long-term exposure. Mansoori et al. [14] found that the corrosion rate, in an electrolyte agitated at 1% *w*/*w* NaCl saturated by $CaCO_3$ (160 ppm Ca^{2+}) and with CO_2 at 80 °C, was lower during the first 60 h of exposure, with respect to the corrosion rate in a medium without $CaCO_3$ (1% NaCl + $NaHCO_3$). After this period, the rate relation was reverted.

A. Shamsa et al. [5] studied the role of Ca^{2+} ions on the CO_2 corrosion of X65 steel in a stagnant medium. For this purpose, tests were conducted at 80 and 150 °C for 96 h using two different solutions, 3% *w*/*w* NaCl and 1.54% *w*/*w* NaCl + 1.83% *w*/*w* $CaCl_2 \cdot H_2O$ to maintain the same Cl^- concentration in both cases. The addition of Ca^{2+} at 80 °C accelerated pit growth and these effects diminished at 150 °C.

Rizzo et al. [15] investigated the effect of Ca^{2+} on an already-formed $FeCO_3$ protective layer on L80-1Cr steel, and its influence on the corrosion behavior in an aqueous solution saturated by CO_2 at 1% *w*/*w* NaCl in 0, 100, 1000, and 10,000 ppm Ca^{2+} (from $CaCl_2 \cdot H_2O$) at atmospheric pressures and at 80 °C under stagnant conditions. Throughout this experience, they observed three stages. During the first stage, the sample was left to corrode until Fe^{2+} ions super-saturated the solution, thus promoting $FeCO_3$ precipitation. This period was characterized by a continuous increase in both potential and corrosion rates. In the second stage (15 h), substrate stabilization was allowed, with stable corrosion potential and corrosion rate values, and low Fe^{2+} concentrations, because of its precipitation. During the third stage, they added Ca^{2+}, observing that, for higher concentrations, this caused the potential to decrease and the corrosion rate to increase.

Li et al. [16] studied the role of Ca^{2+} ions on the CO_2 corrosion of N80 carbon steel in a stagnant medium with bubbling in $CO_2 + N_2$ at 150 °C. To this end, they performed measurements using solutions ranging from 0 to 10,000 ppm Ca^{2+} (from $CaCl_2$) in a medium with the required amount of NaCl, for a fixed Cl^- concentration of 22,009 ppm. They found that the general corrosion rate increased to 0.0180 mm/y when [Ca^{2+}] = 0 ppm and up to 0.3589 ppm when [Ca^{2+}] = 2000 ppm, decreasing to 0.3070 mm/y when [Ca^{2+}] = 10,000 ppm. Without the presence of Ca^{2+}, the formed $FeCO_3$ corrosion film exhibited a relatively good corrosion resistance, confirmed by the lowest corrosion rate.

In view of the above mentioned results, not many works assess the CO_2 corrosion behavior in the presence of calcium ions. They that do incorporate this cation from $CaCl_2$, preferentially; although, some authors used $CaCO_3$ $CaCO_3$. In addition, most of the times, they worked under stagnant conditions. Ca^{2+} ions can be added from different salts by adding chlorides, carbonates, and sulfates, whose presence may alter the metal surface attack. It is worth noting that corrosion processes and the precipitation of corrosion products and/or encrustations are significantly affected by concentration gradients and, thus, by mass transfer between the bulk solution and steel surface [17].

The aim of this study is to investigate the corrosion rate of carbon steel subjected to the attack of electrolytic media saturated with CO_2 at a working temperature of 65 °C under dynamic conditions. The objective is to assess the effect of the Ca^{2+} ion on the corrosion rate and its dependence on the associated anion (Cl^- or $CO_3{}^{2-}$) to that cation. Measurements are also compared to values obtained when Na^+ is incorporated into the medium. All of this is performed to evaluate whether the addition of Ca^{2+} affects the corrosion rate and to what extent this effect is attributed to the cation. Linear polarization-resistance measurements are conducted using a potentiostat/galvanostat coupled with a rotor–stator system in a ring configuration with AISI 1040 Steel, rotating at 600 RPM. Solutions are prepared with different salts added, such as NaCl, $CaCO_3$, Na_2CO_3, and $CaCl_2$, which are saturated with CO_2.

2. Experimental Methods

The corrosive mediums were prepared in the laboratory with pro-analytics reagents and distilled water. The solutions that were used were the following:

- Assay 1: 2% (*w*/*w*) NaCl with 1380 ppm $CaCl_2$ + CO_2;
- Assay 2: 2% (*w*/*w*) NaCl + CO_2;
- Assay 3: 2% (*w*/*w*) NaCl with 1360 ppm Na_2CO_3 + CO_2;
- Assay 4: 2% (*w*/*w*) NaCl with 1.250 g $CaCO_3$ per liter of solution + CO_2;
- Assay 5: Solution with 1450 ppm NaCl + CO_2;
- Assay 6: Solution with 1380 ppm $CaCl_2$ + CO_2;
- Assay 7: Solution with 1360 ppm Na_2CO_3 + CO_2;
- Assay 8: Solution with 500 ppm $CaCl_2$ + CO_2;
- Assay 9: Solution with 424 ppm Na_2CO_3 + CO_2;
- Assay 10: Solution with 1.250 g $CaCO_3$ per liter of solution + CO_2.

At first, NaCl-concentrated solutions were used, as found in the corrosive environment of the co-produced water with oil. Then, other salts were added. Finally, NaCl was removed from the system to assess how salts behaved without its influence. Regarding $CaCO_3$, a super-saturated solution was prepared; however, for the purpose of assessing the solubility of this salt under the conditions of the assay, it was considered as a concentration in a Ca^{2+} solution equal to 180 ppm, in accordance with an estimate average from the work of Plummer and Busenberg [18].

The graduated cylinders for dynamic conditions were manufactured using AISI 1040 steel bars, which were toned into rings with an outer diameter of 15 mm and 5.3 mm in height. The steel samples were water sanded with silicon carbide sandpaper with granulometry values of 240, 320, 400, and 600. The graduated cylinders were cleaned with ethanol and air-dried upon each sandpaper change. Finally, they were cleaned with isopropyl alcohol and then dried. They were kept in a desiccator with silica gel until they were used.

The equipment used for the measurements were a Metrohm potentiostat/galvanostat, PGSTAT204, with its respective NOVA 2.1 software. A PINE rotor stator was used in its ring configuration with a speed of 600 rpm.

A 500 mL glass cell with 3 electrodes was used: a working electrode mounted on a rotating axis, a platinum counter electrode, and an Ag/AgCl (KCl 3M) reference electrode mounted in the front Luggin capillary.

The methodology that was applied was linear polarization resistance (LPR), with a sweep speed of 0.1 mV/s.

The solution was heated to 65 ± 2 °C, which required 1/2 an hour. Before performing the measurement, the carbon dioxide was immersed in the cell for 60 min. During this stage, all electrodes, except the working electrode, were immersed in the solution. After this period, the working electrode was immersed in the medium and, for an hour, the open circuit potential was measured. Then, the linear polarization-resistance test was performed using the open circuit potential ranging from −20 mV to +20 mV. It should be noted that the measurements were performed in duplicate or until an acceptable repeatability was observed between them.

The polarization resistance value (Rp) was used to calculate the corrosion rate, using the Stern–Geary [19] equation (Equation (1)):

$$i_{corr} = \frac{B}{R_p} \quad (1)$$

i_{corr} = corrosion current [mA/cm^2];
B = Stern-Geary coefficient [mV];
R_p = Polarization resistance [Ωcm^2].

In this study, B equals 26 mV, given that it is a value that it is commonly accepted in CO_2 corrosion studies. It is noteworthy that it is not based on specific Tafel slopes, because the corrosion mechanism is not strictly controlled by the mass transfer [14]. The value of B was determined from an adjustment of the current density and weight loss measurements [20–22].

The corrosion rate (CR), measured in mm/y, is calculated using the following equation [23]:

$$CR = K_1 \frac{i_{corr}}{\rho} EW \quad (2)$$

CR = Corrosion rate [mm/yr];
$K_1 = 3.27 \times 10^{-3}$ [mm g/μA cm yr];
P = density [g/cm^3];
EW = Equivalent weight = 27.92.

After measuring, the graduated cylinders were cleaned using ethyl alcohol in an ultrasonic bath, and were kept in a desiccator.

3. Results and Discussion

Figure 1 shows the linear polarization-resistance curves for solutions saturated by CO_2.

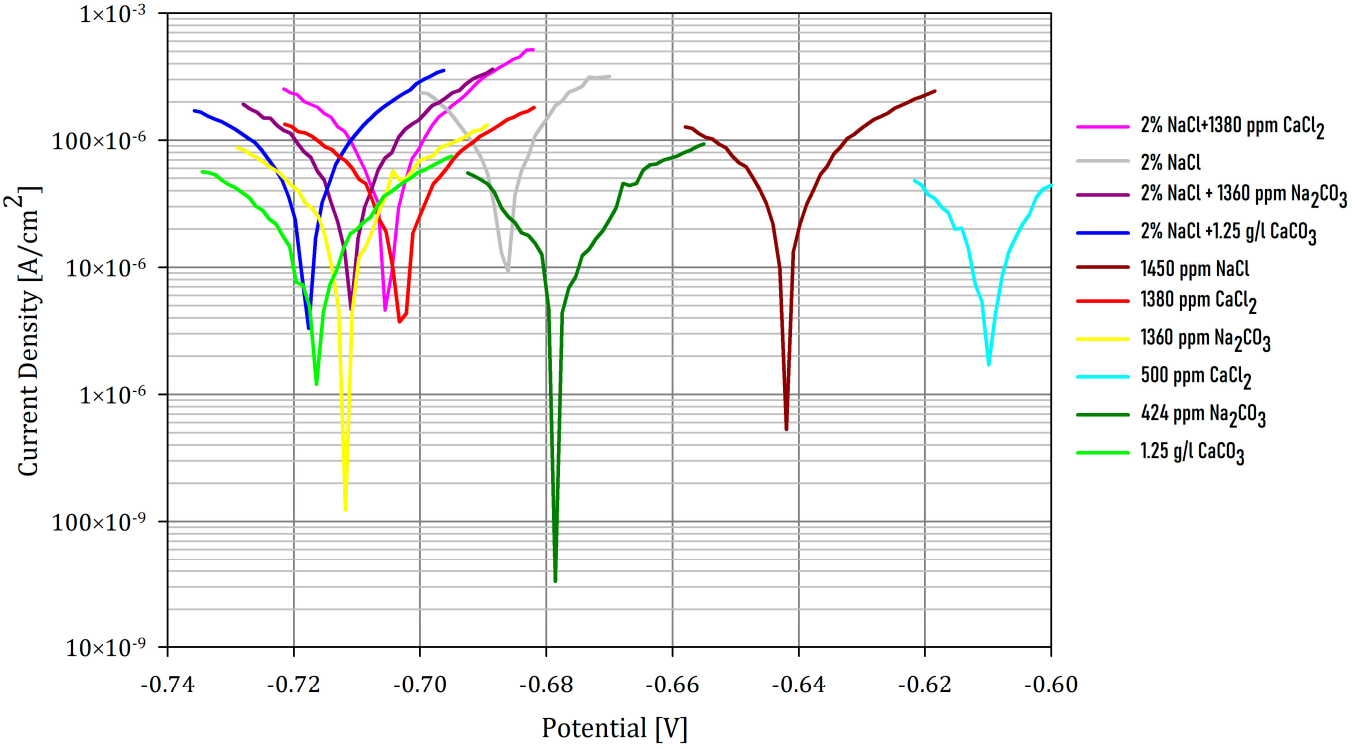

Figure 1. Linear polarization-resistance test, 600 rpm, 65 °C, potentials vs. Ag/AgCl.

Figure 2 shows the curves for the reading of the linear polarization resistance.

Table 1 shows the measured and calculated values for the different mediums.

Siderite ($FeCO_3$) is an isostructural mineral in calcite ($CaCO_3$) and magnesite ($MgCO_3$) regarding the cell parameters (as they crystallize in the same crystal system and the atoms in the unit cell are in the same positions). The specific defects of these isostructural minerals are vacancies and stacking faults, among others [24]. On the other hand, dolomite [$CaMg(CO_3)_2$] also has a crystal structure similar to calcite; however, it exhibits alternate rows of Ca and Mg ions along [42$\bar{1}$] the surface (10$\bar{1}$4). These have been dealt with in studies [25,26] with atomic force microscopy (AFM) applied to calcite, dolomite, and magnesite surfaces in water, through a large-scale atomic/molecular massively parallel simulator (LAMMPS) MD code and free-energy calculations. It was found that water exchange on Ca for dolomite slowed down in a magnitude-order different from calcite. This indicates that a dolomite layer on the steel surface is more protective than a calcite layer, because the latter dissolves faster in an aqueous medium. Due to the structural similarity between dolomite and ankerite [$CaFe(CO_3)_2$] [27,28], which are almost identical, we can infer from the corrosion point of view that an ankerite layer formed on the steel surface is more protective

than a calcite and/or siderite layer, since the former two are isostructural. This conjecture is verified in Table 1, assay 10, where CR is the lowest at 0.97 mmpy due to ankerite formation. In these assays, carbon steel is in contact with CO_2 and $CaCO_3$, Fe (II) slows down calcite growth by blocking the growth sites and incorporating into $CaCO_3$ [29–32].

Table 1. Measurements vs. Ag/AgCl and calculations at 65 °C, 600 rpm, and saturated CO_2.

Sample	NaCl [ppm]	$CaCO_3$ [ppm]	$CaCl_2$ [ppm]	Na_2CO_3 [ppm]	pH	Rp [Ω]	Ecorr [mV]	i [μA/cm^2]	CR [mmpy]
1	20,000	-	1380	-	4.07	23	−704	463	5.38
2	20,000	-	-	-	4.38	25	−686	431	5.01
3	20,000	-	-	1360	6.74	28	−712	379	4.41
4	20,000	1250	-	-	5.71	31	−719	349	4.06
5	1450	-	-	-	4.04	47	−644	223	2.59
6	-	-	1380	-	4.03	53	−703	201	2.34
7	-	-	-	1360	6.75	68	−712	156	1.81
8	-	-	500	-	4.12	87	−611	121	1.41
9	-	-	-	424	6.34	98	−678	101	1.29
10	-	1250	-	-	5.97	126	−715	84	0.97

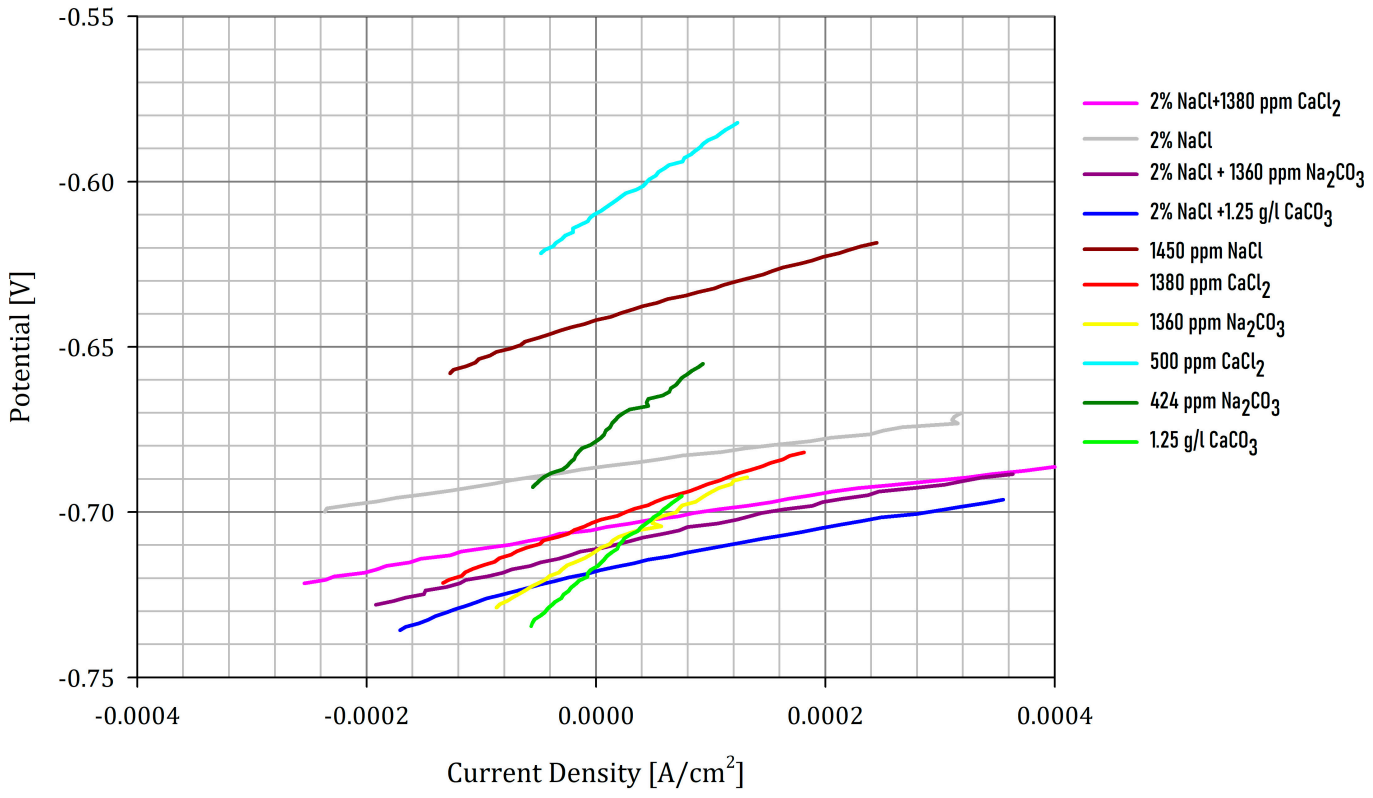

Figure 2. Graph for the linear polarization-resistance calculations.

Muruta et al. [2], using synthetic seawater at 60 °C and 1 atm of CO_2, found depositions on a carbon steel surface, such as $FeCO_3$, $CaCO_3$, and α, $\gamma \bullet Fe_2O_3 \bullet H_2O$, which were identified using X-ray diffraction analysis. On the other hand, Hausler [33] assumed $FeCO_3$ to be an n-type semiconductor with a transport mechanism of iron through intersti-

tials, thus explaining the CO_2 corrosion mechanism for AISI 1018. In this mechanism, the corrosion relation involved is:

$$Fe^0 \leftrightarrow \left[Fe^{2+}\right] + 2e^- \quad (3)$$

[ ] represents interstitial ions, indicating that iron oxidation leads to interstitial iron ions and an excess of electrons in the $FeCO_3$ encrustations. By applying the law of mass action to Equation (3), Equation (4) is obtained:

$$K = \left[Fe^{2+}\right] e^2 \quad (4)$$

where the product of interstitial ion and electron square concentrations must be constant. It is reasonable to assume that protons can be incorporated into the encrustation through the protonation of carbonate ions in the system. This leads to iron ion vacancies that, in turn, lead to a higher concentration of interstitial iron ions and, thus, to a greater encrustation permeability [33]. Hausler stated that a cation, such as protons, is introduced into the system; by analogy, in our work, we hold that the Na^+ cation behaves in a similar way, generating specific defects in the crystal system and favoring a higher porosity in the corrosion products.

In our work, conducted under dynamic conditions with a cylinder rotating at 600 rpm at 65 °C and saturated by CO_2, we found the following decreasing order in the carbon steel corrosion rate:

2% NaCl + 1380 ppm $CaCl_2$ > 2% NaCl > 2% NaCl + 1360 ppm Na_2CO_3 > 2% NaCl + 1.25 g/L $CaCO_3$ > 1450 ppm of NaCl > 1380 ppm $CaCl_2$ > 1360 ppm Na_2CO_3 > 500 ppm $CaCl_2$ > 424 ppm Na_2CO_3 >> 1.25 g/L $CaCO_3$.

Chlorides favor the carbon steel corrosion process due to their affinity of this anion to iron, especially in an acidic medium. In our case study, the pH of the solution with 2% NaCl saturated by CO_2 at atmospheric pressure is 4.4. Additionally, it is well-known that solutions containing CO_2 in contact with low-alloy steel create a corrosion product protective layer on the material, basically formed by siderite ($FeCO_3$) [34,35]; however, the presence of certain ions, essentially chlorides, interfere with the formation of the protective layer, causing its dissolution [36] and resulting in an increase in the corrosion rate. Moreover, the presence of Na^+ promotes the action of chlorides. A plausible explanation for the corrosion rate increase is that Na^+ ions from NaCl in solution are incorporated into the crystal system of $FeCO_3$, creating new crystal defects, Na^+ ions, placing themselves in interstitial positions and creating Fe^{2+} vacancies to keep the electroneutrality of the siderite [37,38]. In accordance with the above mentioned results, a simplified sequence of the reactions with a pH < 4.5 might be:

$$2\,NaCl + CO_2 + H_2O \rightarrow 2\,HCl + Na_2CO_3 \quad (5)$$

$$(1 - x)\,FeCO_3 + xNa_2CO_3 \rightarrow Fe_{(1-x)}\square_x[Na_{2x}]CO_3 \quad (6)$$

where $\square$ are Fe^{2+} vacancies and [ ] are Na^+ interstitial ions.

This contamination mechanism of the siderite crystals in the presence of NaCl leads to the instability of the protective layer, making it porous and increasing the Fe^{2+} dissolution in the solution. This can be seen in Table 1; when only NaCl is apparent, the pH is acidic and CR is equal to 5.01 mmpy, showing the effect, first by Equation (5) and supported by Equation (6). However, when NaCl + Na_2CO_3 is present, CR is equal to 4.41 mmpy (assay 3), which leads us to think that the reaction mechanism is deactivated, mainly because the reaction of Equation (5) is inhibited. This can be confirmed when we consider that, when NaCl is absent (assay 7), CR is equal to 1.81 mmpy.

It was also observed that as the Na_2CO_3 concentration decreased, CR decreased from 1.81 (assay 7) to 1.29 mmpy (assay 9), even though the pH decreased, which confirmed that a lower availability of Na^+ to create vacancies led to the decrease in CR.

Although there was a decrease in the corrosion rate when the Cl^- concentration decreased (CR assay 1 > CR assay 2 > CR assay 5; CR assay 6 > CR assay 8), at the same concentration of Cl^-, we observed that CR was higher in NaCl than in $CaCl_2$, as shown by assays 5 and 6. This reinforces the fact that siderite crystals are unstable in the presence of NaCl due to the incorporation of Na^+ into the deposition and the subsequent vacancy generation; but, in presence of Ca^{2+}, the formation of ankerite becomes possible, which is much more stable and, is thus better for protecting against corrosion.

Following our reasoning and applying it to ankerite, we can argue that the increase in the corrosion rate is due to Na^+ ions incorporating into the crystal system of $CaFe(CO_3)_2$, creating new crystal defects; the Na^+ ions place themselves in interstitial positions and create vacancies of Ca^{2+} and/or Fe^{2+} to keep the electroneutrality of the deposition. In line with the above:

$$(1-x)\,FeCO_3 + xNa_2CO_3 + \,yCaCO_3 \rightarrow Fe_{(1-x)}\square_x\left[Ca_yNa_{2x}\right](CO_3)_{1+y} \quad (7)$$

$$(1-x)\,CaCO_3 + xNa_2CO_3 + \,yFeCO_3 \rightarrow Ca_{(1-x)}\square_x\left[Fe_yNa_{2x}\right](CO_3)_{1+y} \quad (8)$$

where Na_2CO_3 is obtained from the reaction shown by Equation (5), □ are the Ca^{2+} or Fe^{2+} vacancies, and [ ] are interstitial ions.

This can be observed by comparing assay 10, with a CR of 0.97 mmpy due to the formation of ankerite, which, by adding NaCl (assay 4) increases its CV to 4.06 mmpy because it leads to the formation of corrosion products, such as the ones indicated by Equation (7) or Equation (8), and continues to increase up to 5.01 mmpy with assay 2, even though it has the lowest total salt concentration. These results coincide with the ones obtained by Tavares et al. [6], who studied the effects of Ca^{2+} ions on the CO_2 corrosion of API 5L-Gr B steel by measuring it in two mediums saturated by NaCl and by CO_2 in the presence and absence of $CaCO_3$. Therefore, the Ca^{2+} cation also has a passivizing effect on corrosion in the absence of NaCl.

If we observe the results in Table 1, we can see that the role that the Ca^{2+} cation plays against corrosion is influenced by the associated anion. In the absence of NaCl, the corrosion rate of AISI 1040, under the conditions that are tested herein, is higher when the Ca^{2+} cation has Cl^- as its anion instead of $CO_3{}^{2-}$. This can be verified by comparing assays 8 and 10, which have the same Ca^{2+} concentrations in solution and a CR of 1.41 mmpy when working with $CaCl_2$, while it decreases to 0.97 mmpy when working with $CaCO_3$. This is because chloride ions, similar to an acidic pH, can destroy the passivation layer [39]. To sum up, the absence of chlorides improves the encrustation protectiveness against corrosion, and ankerite is formed when working with $CaCO_3$.

4. Conclusions

The corrosion rate in the presence of Ca^{2+} depends on the associated anion (Cl^- or $CO_3{}^{2-}$) from which it is added to the solution, whether or not NaCl is present. Ca^{2+} ion passivizes carbon steel, especially in NaCl-free mediums.

Ca^{2+} associated with the $CO_3{}^{2-}$ anion has a passivation effect that cannot be evinced by Na^+ associated with the same anion, due to the formation of an ankerite layer in the absence of NaCl in the medium.

Although the corrosion rate of a low-alloy steel increases along with the chloride concentration, when it is equal to the concentration of this anion, the corrosion rate depends on the accompanying cation (Na^+ or Ca^{2+}), from which the chloride is incorporated.

Author Contributions: Conceptualization, G.L.B.; methodology, V.V.A. and G.L.B.; validation, V.V.A.; investigation, V.V.A.; resources, V.V.A. and G.L.B.; data curation, V.V.A. and G.L.B.; writing—original draft preparation, V.V.A.; writing—review and editing, V.V.A. and G.L.B. All authors have read and agreed to the published version of the manuscript.

Funding: This work was supported by TECTIONS SOUTH S.A.

Institutional Review Board Statement: Not applicable.

Informed Consent Statement: Not applicable.

Data Availability Statement: Not applicable.

Conflicts of Interest: The authors declare no conflict of interest.

References

1. Wu, S.L.; Cui, Z.D.; He, F.; Bai, Z.Q.; Zhu, S.L.; Yang, X.J. Characterization of the surface film formed from carbon dioxide corrosion on N80 steel. *Mater. Lett.* **2004**, *58*, 1076–1081. [CrossRef]
2. Murata, T.; Sato, E.; Matsuhashi, R. Factors Controlling Corrosion of Steels in CO_2 Saturated Environments. In *Advances in CO_2 Corrosion in the Oil and Gas Htdustty, Proceedings of the Corrosion 83 Symposium, Anaheim, CA, USA, 18–19 April 1983*; Hausler, R.H., Ed.; National Association of Corrosion Engineers (NACE): Houston, TX, USA, 1983; Volume 1.
3. De Motte, R.A.; Barker, R.; Burkle, D.; Vargas, S.M.; Neville, A. The Early Stages of $FeCO_3$ Scale Formation Kinetics in CO_2. Corrosion. *Mater. Chem. Phys.* **2018**, *216*, 102–111. [CrossRef]
4. Ma, Z.; Yang, Y.; Brown, B.; Nesic, S.; Singer, M. Investigation of Precipitation Kinetics of $FeCO_3$ by EQCM. *Corros. Sci.* **2018**, *141*, 195–202. [CrossRef]
5. Shamsa, A.; Barker, R.; Hua, Y.; Barmatov, E.; Hughes, T.L.; Neville, A. The role of Ca^{2+} ions on Ca/Fe carbonate products on X65 carbon steel in CO_2 corrosion environments at 80 and 150 °C. *Corros. Sci.* **2019**, *156*, 58–70. [CrossRef]
6. Mansoori, H.; Young, D.; Brown, B.; Singer, M. Influence of calcium and magnesium ions on CO_2 corrosion of carbon steel in oil and gas production systems-a review. *Nat. Gas Sci. Eng.* **2018**, *59*, 287–296. [CrossRef]
7. Jiang, X.; Zheng, Y.G.; Qu, D.R.; Ke, W. Effect of calcium ions on pitting corrosion and inhibition performance in CO_2 corrosion of N80 steel. *Corros. Sci.* **2006**, *48*, 3091–3108. [CrossRef]
8. Ding, C.; Gao, K.W.; Chen, C.F. Effect of Ca^{2+} on CO_2 corrosion properties of X65 pipeline steel. *Int. J. Miner. Metall. Mater.* **2009**, *16*, 661–666.
9. Tavares, L.M.; da Costa, E.M.; de Oliveira Andrade, J.J.; Hubler, R.; Huet, B. Effect of calcium carbonate on low carbon steel corrosion behavior in Effect of calcium carbonate on low carbon steel corrosion behavior in. *Appl. Surf. Sci.* **2015**, *359*, 143–152. [CrossRef]
10. Navabzadeh Esmaeely, S.; Choi, Y.S.; Young, D.; Nešić, S. Effect of Calcium on the Formation and Protectiveness of Iron Carbonate Layer in CO_2 Corrosion. *Corrosion* **2013**, *69*, 912–920. [CrossRef]
11. Esmaeely, S.N.; Young, D.; Brown, B.; Nešić, S. Effect of Incorporation of Calcium into Iron Carbonate Protective Layers in CO_2 Corrosion of Mild Steel. *Corrosion* **2017**, *73*, 238–246. [CrossRef]
12. Sontvedt, T.; Eriksrud, N. *Effect of Flow on CO_2 Corrosion Rates in Real and Synthetic Formation Waters*; National Association of Colleges and Employers (NACE): Bethlehem, PA, USA, 1987; Volume 1, pp. 20–38.
13. Zhao, G.X.; Li, J.P.; Hao, S.M.; Lu, X.H.; Li, H.L. Effect of Ca^{2+} and Mg^{2+} on CO_2 corrosion behavior of tube steel. *J. Iron Steel Res. Int.* **2005**, *12*, 38–42.
14. Mansoori, H.; Young, D.; Brown, B.; Nesic, S.; Singer, M. Effect of $CaCO_3$-saturated solution on CO_2 corrosion of mild steel explored in a system with controlled water chemistry and well-defined mass transfer conditions. *Corros. Sci.* **2019**, *158*, 108078. [CrossRef]
15. Rizzo, R.; Gupta, S.; Rogowska, M.; Ambat, R. Corrosion of carbon steel under CO_2 conditions: Effect of $CaCO_3$ precipitation on the stability of the $FeCO_3$ protective layer. *Corros. Sci.* **2020**, *162*, 108214. [CrossRef]
16. Li, J.; Sun, C.; Roostaei, M.; Mahmoudi, M.; Fattahpour, V.; Zeng, H.; Luo, J.L. Role of Ca^{2+} in the CO_2 corrosion behavior and film characteristics of N80 steel and electroless Ni–P coating at high temperature and high pressure. *Mater. Chem. Phys.* **2021**, *267*, 124618. [CrossRef]
17. Nesic, S. Effects of multiphase flow on internal CO_2 corrosion of mild steel pipe lines. *Energy Fuels Am. Chem. Soc.* **2012**, *26*, 4098–4111. [CrossRef]
18. Plummer, L.N.; Busenberg, E. The solubilities of calcite, aragonite an vaterite in CO_2-H_2O solutions between 0 and 90 °C, and an evaluation of aqueous model for the system $CaCO_3$-CO_2-H_2O. *Geochim. Cosmochim.* **1982**, *46*, 1011–1040. [CrossRef]
19. Stern, M.; Geary, A.L. Electrochemical Polarization I. A Theoretical Analysis of the Shape of Polarization Curves. *J. Electrochem. Soc.* **1957**, *104*, 56–63. [CrossRef]
20. Sani, F.M.; Brown, B.; Belarbi, Z.; Nesic, S. *An Experimental Investigation on the Effect of Salt Concentration on Uniform CO_2 Corrosion*; Corrosion; Paper Nº 13026; NACE International: Houston, TX, USA, 2019.
21. Yanga, Y.; Browna, B.; Nešić, S.; Gennarob, M.E.; Molinas, B. *Mechanical Strength and Removal of a Protective Iron Carbonate Layer Formed on Mild Steel in CO_2 Corrosion*; Paper No. 10383; NACE International: Houston, TX, USA, 2010.
22. Di Bonaventura, M.; Brown, B.; Nešić, S.; Singer, M. *Effect of Flow and Steel Microstructure on the Formation of Iron Carbonate*; Paper No. 11179; NACE International: Houston, TX, USA, 2018.
23. *ASTMG102*; Standard Practice for Calculation of Corrosion Rates and Related Information from Electrochemical Measurements. ASTM International: West Conshohocken, PA, USA, 2015.

24. Gomez-Villalba, L.S.; López-Arce, P.; Alvarez de Buergo, M.; Fort, R. Atomic Defects and Their Relationship to Aragonite-Calcite Transformation in Portlandite Nanocrystal Carbonation. *Cryst. Growth Des.* **2012**, *12*, 4844–4852. [CrossRef]
25. Reischl, B.; Raiteri, P.; Gale, J.D.; Rohl, A.L. Atomistic Simulation of Atomic Force Microscopy Imaging of Hydration Layers on Calcite, Dolomite, and Magnesite Surfaces. *J. Phys. Chem.* **2019**, *123*, 14985–14992. [CrossRef]
26. Söngen, H.; Reischl, B.; Miyata, K.; Bechstein, R.; Raiteri, P.; Rohl, A.L.; Gale, J.D.; Fukuma, T.; Kühnle, A. Resolving point defects in the hydration structure of calcite (10.4) with three-dimensional atomic force microscopy. *Phys. Rev. Lett.* **2018**, *120*, 116101. [CrossRef]
27. Ross, N.L.; Reeder, R.J. High-pressure structural study of dolomite and ankerite. *Am. Mineral.* **1992**, *77*, 412–421.
28. Chuliá-Jordán, R.; Santamaria-Perez, D.; Ruiz-Fuertes, J.; Otero-de-la-Roza, A.; Popescu, C. Compressibility and Phase Stability of Iron-Rich Ankerite. *Minerals* **2021**, *11*, 607. [CrossRef]
29. Meyer, M. The influence of impurities on the growth rate of calcite. *J. Cryst. Growth* **1984**, *66*, 639–646. [CrossRef]
30. De Leeuw, N.H. Molecular Dynamics Simulations of the Growth Inhibiting Effect of Fe^{2+}, Mg^{2+}, Cd^{2+}, and Sr^{2+} on Calcite Crystal Growth. *J. Phys. Chem. B* **2002**, *106*, 5241–5249. [CrossRef]
31. Mettler, S.; Wolthers, M.; Charlet, L.; Von Gunten, U. Sorption and catalytic oxidation of Fe(II) at the surface of calcite. *Geochim. Cosmochim. Acta* **2009**, *73*, 1826–1840. [CrossRef]
32. Gutjahr, A.; Dabringhaus, H.; Lacmann, R. Studies of the growth and dissolution kinetics of the $CaCO_3$ polymorphs calcite and aragonite. The influence of divalent cation additives on the growth and dissolution rates. *J. Cryst. Growth* **1996**, *158*, 310–315. [CrossRef]
33. Hausler, R.H. (Ed.) The mechanism of CO_2 corrosion steel in hot, deep gas wells. In *Advances in CO_2 Corrosion in the Oil and Gas Htdustty, Proceedings of the Corrosion 83 Symposium, Anaheim, CA, USA, 18–19 April 1983*; National Association of Corrosion Engineers (NACE): Houston, TX, USA, 1983; Volume 1.
34. Alsalem, M.M.; Camilla, S.; Ryan, M.P.; Campbell, K.S. Understanding the Role of NaCl Concentration on the Corrosion of Carbon Steel and $FeCO_3$ Formation in CO_2 Containing Electrolytes. *Ind. Eng. Chem. Res.* **2021**, *60*, 12032–12048. [CrossRef]
35. Zhang, D.; Gao, X.; Li, W.; Li, B.; Guo, J.; Zhang, J.; Pang, Q.; Xu, Z. CO_2 corrosion behavior of high-strength martensitic steel for marine riser exposed to CO_2 saturated salt solution. *Mater. Res. Express* **2021**, *8*, 076517. [CrossRef]
36. Jiang, X.; Nešic, S.; Huet, F. The Effect of Electrode Size on Electrochemical Noise Measurements and the Role of Chloride on Localized CO_2 Corrosion of Mild Steel. In Proceedings of the CORROSION 2009, Atlanta, GA, USA, 22–26 March 2009; NACE International: Houston, TX, USA, 2009.
37. Ishikawa, M.; Ichikuni, M. A Model of Crystal Defects in Calcita by Sodium and Potassium Uptake. *Bull. Chem. Soc. Jpn.* **1986**, *59*, 3809–3814. [CrossRef]
38. Ishikawa, M.; Ichikuni, M. Uptake of sodium and potassium by calcite. *Chem. Geol.* **1984**, *42*, 137–146. [CrossRef]
39. Duffó, G.S.; Farina, S.B. *La Corrosión de Estructuras de Hormigón Armado: Principios Básicos, Monitoreo y Prevención*; Editorial Académica Española: Berlín, Germany, 2016.